

# Emergence of a renormalized $1/N$ expansion in quenched critical many-body systems

Benjamin Geiger, Juan Diego Urbina, and Klaus Richter

*Institut für Theoretische Physik, Universität Regensburg, D-93040 Regensburg, Germany*

(Dated: October 16, 2020)

We consider the fate of  $1/N$  expansions when a many-body quantum system is quenched across criticality and show the emergence of  $e^{2\lambda t}/N$  as renormalized parameter ruling the quantum-classical transition and accounting non-perturbatively for the local divergence rate  $\lambda$  of mean-field solutions. In terms of  $e^{2\lambda t}/N$ , quasiclassical expansions of paradigmatic examples of criticality like the self-trapping transition in an integrable Bose-Hubbard dimer and the generic instability of attractive bosonic systems towards soliton formation, are pushed to arbitrarily high orders. The agreement with numerical simulations supports the general nature of our results in the appropriately combined long-time  $\lambda t \rightarrow \infty$  quasiclassical  $N \rightarrow \infty$  regime, out of reach of expansions in the bare parameter  $1/N$ . For scrambling in many-body hyperbolic systems, our results provide formal grounds to a conjectured multi-exponential form of out-of-time-ordered correlators.

The semiclassical (small  $\hbar$ ) expansion provides a tool to address in a systematic way quantum effects on observables admitting a power expansion around their classical values where  $\hbar = 0$  [1, 2]. It comes as no surprise then that such expansions have achieved a prominent role in the study of both the quantum-classical transition itself [3] and the physics of systems in the mesoscopic regime [4, 5]. With the impressive advances in the coherent preparation, control and manipulation of ever larger quantum systems, this mesoscopic regime where the system remains coherent but where typical classical actions are large compared with  $\hbar$  keeps growing, and with it the range of applications of these methods [6]. The extensive use of phase space methods based on Wigner-Moyal calculus in its several variants, like high-temperature expansions in statistical mechanics [1, 7, 8], Truncated Wigner approximation describing the dynamics of cold atoms [9–12], Weyl-Kirkwood expansions in nuclear physics [5, 13] and others, show the broadness and power of quasiclassical expansions [14].

When lifted into the realm of interacting many-body systems admitting a well defined mean-field description in terms of bosonic order parameters, the quasiclassical expansion is formally constructed by means of the key identification of the number of particles  $N$  as inverse effective Planck constant, namely  $\hbar_{\text{eff}} = 1/N$ , where quantum fluctuations around the mean field limit assume the form of expansions in powers of  $1/N$  [15–18]. In particular, matrix elements of time-dependent operators in the Heisenberg picture are expected to have an (at least asymptotic)  $1/N$  expansion. The limitations of such a bare large- $N$  expansion become evident when the dynamics of the observables is driven by a quench across a phase transition [19], here defined as an instability of the mean-field when changing a control parameter [18, 20–26]. The interplay between local mean field instability, measured by an imaginary Bogoliubov frequency  $\lambda$ , and quantum fluctuations makes the Wigner-Moyal expansion valid only before the onset of non-perturbative quantum interference effects [27] at a time scale  $t_E \sim \log N/(2\lambda)$

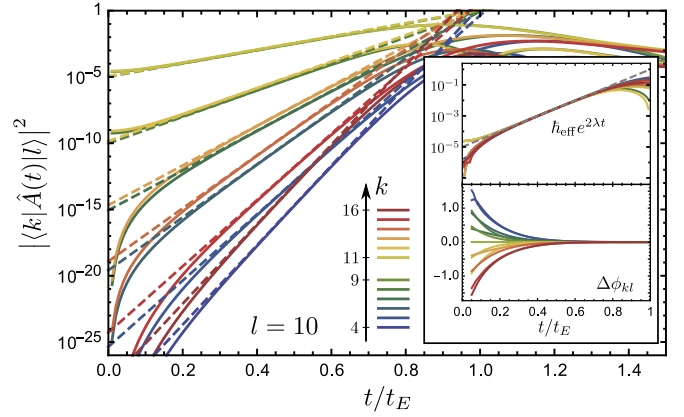


FIG. 1. Exponential growth of matrix elements, Eq. (1), with  $\hat{A} = \hat{z} + \hat{z}^2$  after an interaction quench from  $\alpha = 0$  to  $\alpha = 2.5$  for  $N = 10^5$  particles in the Bose-Hubbard dimer [Eqs. (2,3),  $\hat{z} = (\hat{n}_1 - \hat{n}_2)/2N$ ]. The main panel shows the absolute squares for  $l = 10$  and  $k \neq l$  ranging from 4 to 16. Solid lines represent the numerical data while the dashed lines show the predicted dominant scaling, Eq. (1). The inset shows a collapse of the absolute values (top) and the phases (bottom) using the prediction for the coefficients  $c_{kl}$ .

[28, 29] parametrically small in  $N$ . In practice, however, the quasiclassical expansion (and its characteristic Taylor-like form in  $t$  and  $1/N$ ) breaks down well before this fundamental limitation due to the uncontrolled complexity of high-order Moyal expansions.

In this paper we address this early breakdown of  $1/N$  expansions around mean-field instabilities, and show that it can be pushed up to  $t \sim t_E$  by introducing a renormalized small parameter that subsumes the effect of local hyperbolicity. We analytically show that, in a suitable basis, matrix elements of perturbed Heisenberg operators in the regime  $\lambda t \gg 1, N \rightarrow \infty$ , satisfy the scaling

$$\langle k|\hat{A}(t)|l\rangle \sim c_{kl} \left( e^{\lambda t}/\sqrt{N} \right)^{|k-l|} = c_{kl} e^{\lambda(t-t_E)|k-l|}, \quad (1)$$

with  $N$ -independent constants  $c_{kl}$ . Beyond the shortest time scale  $1/\lambda$  (often associated with single-particle

scattering or relaxation) matrix elements exponentially increase, shifted by  $t_E$ . This general prediction provides the precise way how  $t$  and  $N$  commonly determine this increase, effectively absorbing the effect of local mean-field instability within the  $1/N$  expansion in a single, renormalized expansion parameter. Equation (1) is compared against extensive numerical simulations for the paradigmatic case of the self-trapping transition in the integrable Bose-Hubbard dimer [16, 30, 31] in Fig. 1. Later, we will report similar results for the nonintegrable trimer [32–34] with close relation to the generic instability of attractive Bose gases towards soliton formation [35, 36].

Our analysis is based on the generic behaviour of time-dependent perturbative expansions of interacting bosonic systems applied to a quench around criticality. It is illustrated for definiteness using the two-site Bose-Hubbard model defined by the Hamiltonian

$$\hat{H} = -J \left[ \hat{a}_1^\dagger \hat{a}_2 + \hat{a}_2^\dagger \hat{a}_1 \right] + \frac{U}{2} \left[ (\hat{a}_1^\dagger)^2 (\hat{a}_1)^2 + (\hat{a}_2^\dagger)^2 (\hat{a}_2)^2 \right]. \quad (2)$$

It allows for a detailed analysis due to its low level of complexity, while generalization to an arbitrary number of sites can be found in [37]. The steps of the calculation are the same in all cases: First, a mean-field (MF) model has to be identified as a formal classical limit, using the (conserved) inverse particle number as an effective Planck constant. Then, an expansion of the MF Hamiltonian around the pre-quench global minimum is used to obtain a well-controlled low-energy description of the system via canonical quantization. An expansion of the post-quench unstable dynamics around the very same point is then the starting point for a perturbative analysis that finally reveals the renormalized expansion parameter, leading to the scaling in Eq. (1).

*Quantization of the mean field* — As the particle number  $N$  is conserved, the MF dynamics is described using the occupation imbalance and the conjugate phase only, leading to the energy per particle [37]

$$\frac{H_{\text{MF}}}{\tilde{N}J} = h(z, \varphi) - 1 - \alpha \left( \frac{1}{2} + \frac{1}{\tilde{N}} - \frac{1}{\tilde{N}^2} \right) \quad (3)$$

with the classical MF dynamics only determined by the Josephson Hamiltonian

$$h(z, \varphi) = 1 - \sqrt{1 - 4z^2 \cos \varphi} - 2\alpha z^2. \quad (4)$$

In Eqs. (3) and (4),  $z = (n_1 - n_2)/(2\tilde{N})$  is the relative occupation imbalance, with  $\tilde{N} = N + 1 \approx N$ ,  $\varphi$  is the conjugate phase, and the interaction is scaled as  $\alpha = -U\tilde{N}/2J$  with  $\alpha > 0$  for attractive coupling. The global energy minimum at  $z = \varphi = 0$  for couplings  $\alpha \leq 1$  is replaced by a hyperbolic fixed point for  $\alpha > 1$ .

We first consider the quadratic approximation of Eq. (4) around the global minimum for  $\alpha < 1$ , described by a harmonic oscillator

$$h_0(z, \varphi) = \frac{\varphi^2}{2} + \frac{\omega^2 z^2}{2}, \quad \omega = 2\sqrt{1 - \alpha}. \quad (5)$$

The states  $|k\rangle$  in Eq. (1) are thus harmonic oscillator states. For  $\alpha > 1$  one has

$$h(z, \varphi) = \frac{\varphi^2}{2} - \frac{\lambda^2 z^2}{2} + v(z, \varphi) \quad (6)$$

with  $v$  at least cubic in  $(z, \varphi)$  and

$$\lambda = 2\sqrt{\alpha - 1} \quad (7)$$

being the instability of the hyperbolic fixed point.

The MF Hamiltonians (5) and (6) are then quantized by replacing the variables  $z, \varphi$  by operators (using symmetric ordering) and requiring the commutator relation

$$[\hat{z}, \hat{\varphi}] = i\hbar_{\text{eff}} = \frac{i}{\tilde{N}}. \quad (8)$$

*Interaction picture* — Using the interaction picture

$$\hat{A}(t) = e^{\frac{i}{\hbar_{\text{eff}}}(\hat{h}-\hat{v})} \hat{A} e^{-\frac{i}{\hbar_{\text{eff}}}(\hat{h}-\hat{v})}, \quad (9)$$

we treat the post-quench dynamics generated by the quadratic part of  $\hat{h} = h(\hat{z}, \hat{\varphi})$  exactly. A Heisenberg operator (denoted with subindex  $H$ ) can then be formally expanded as [38]

$$\hat{A}_H(t) = \sum_{n=0}^{\infty} \frac{1}{(i\hbar_{\text{eff}})^n} \int_0^t dt_1 \int_0^{t_1} dt_2 \cdots \int_0^{t_{n-1}} dt_n \quad (10)$$

$$[[\dots [[\hat{A}(t), \hat{v}(t_1)], \hat{v}(t_2)], \dots], \hat{v}(t_n)],$$

where the zero-order term is defined as  $\hat{A}(t)$ . Equation (10) can be used as a perturbation expansion when both  $\hat{z}$  and  $\hat{\varphi}$  can be considered as small, as is the case for the pre-quench eigenstates that have a characteristic extent  $\sim \sqrt{\hbar_{\text{eff}}}$  in both  $z$  and  $\varphi$ . We make this explicit by defining the hermitian quadrature-like operators

$$\hat{b}_{\pm} = \frac{1}{\sqrt{2\lambda\hbar_{\text{eff}}}} (\lambda\hat{z} \pm \hat{\varphi}), \quad [\hat{b}_-, \hat{b}_+] = i, \quad (11)$$

with a trivial time evolution  $\hat{b}_{\pm}(t) = e^{\pm\lambda t} \hat{b}_{\pm}(0)$ . They are related to the pre-quench ladder operators of Eq. (5), by

$$\hat{b}_{\pm} = \frac{e^{\mp i\phi} \hat{a} + e^{\pm i\phi} \hat{a}^\dagger}{\sqrt{2 \sin 2\phi}}, \quad \hat{a}|k\rangle = \sqrt{k}|k-1\rangle, \quad (12)$$

with  $\phi = \tan^{-1}(\omega/\lambda)$ , such that they are  $\mathcal{O}(\hbar_{\text{eff}}^0)$  when applied to the noninteracting states with  $k = \mathcal{O}(N^0)$ , i.e. the states with quantum fluctuations  $\langle \hat{b}_{\pm}^2 \rangle = \mathcal{O}(\hbar_{\text{eff}}^0)$ .

With these definitions, one can formally use  $\hbar_{\text{eff}}$  as a small parameter and the condition for the validity of the expansion (10) is given by a *local* Ehrenfest time

$$\hbar_{\text{eff}} \langle \hat{b}_{\pm}^2(t) \rangle \ll 1 \quad \Leftrightarrow \quad t \ll \frac{\log(\hbar_{\text{eff}}^{-1})}{2\lambda} \equiv t_E, \quad (13)$$

characterized by the breakdown of the quadratic approximation. The expectation value can be taken in the

ground state or in a thermal ensemble of the pre-quench system with temperature  $k_B T / \Delta = \mathcal{O}(\hbar_{\text{eff}}^0)$ , where  $\Delta$  is the single- or quasi-particle excitation energy.

The explicit time dependence of  $\hat{v}(t)$  takes the form

$$\hat{v}(t) = \sum_{\mu, \nu} v_{\mu\nu} \hbar_{\text{eff}}^{\frac{\mu+\nu}{2}} e^{(\nu-\mu)\lambda t} \left\{ \hat{b}_-^\mu \hat{b}_+^\nu \right\}_s, \quad (14)$$

where the dependence on  $\hbar_{\text{eff}}$  has been made also explicit and  $\{\dots\}_s$  denotes symmetric ordering. The same can be done for  $\hat{A}(t)$ , assuming that the MF limit of  $\hat{A}(0)$  is independent of  $\hbar_{\text{eff}}$  [39], such that the time-dependence (and the coefficients  $v_{\mu\nu}$ ) can be pulled out of the commutators in Eq. (10) that is now organized as a power series in  $\sqrt{\hbar_{\text{eff}}}$ . By suppressing corrections of the form  $t e^{-\lambda t}$  for  $t \gg 1/\lambda$  in the respective (operator valued) coefficients one finds the dominant scaling [37]

$$\hat{A}_H(t) \sim \sum_k C_k \left( \sqrt{\hbar_{\text{eff}}} e^{\lambda t} \hat{b}_+ \right)^k \quad (15)$$

with the  $\hbar_{\text{eff}}$ -independent coefficients  $C_k$  determined by the operators  $\hat{A}$  and  $\hat{v}$ . Equation (12) implies

$$\langle k | \hat{b}_+^n | l \rangle = 0 \quad \text{for } n < |k - l|, \quad (16)$$

such that matrix elements scale as stated in Eq. (1) with  $c_{kl} = C_{|k-l|} \langle k | \hat{b}_+^{|k-l|} | l \rangle$  for  $t \ll t_E$ , with possible exceptions only if  $C_{|k-l|} = 0$  for specially constructed operators  $\hat{A}$ .

Nonlinearities of the pre-quench system, Eq. (4) for  $\alpha < 1$ , can now be included in a consistent way: The full eigenstates are expanded in a perturbation series around the harmonic oscillator states  $|k\rangle$ . One can then show using adiabatic switching [37] that these corrections do not contribute to the dominant scaling in Eq. (1), justifying the harmonic approximation, Eq. (5).

Figure 1 shows a comparison of the numerical simulations and the prediction in Eq. (1) for  $N = 10^5$  particles and  $\alpha = 2.5$  using the operator  $\hat{A} = \hat{z} + \hat{z}^2$ . The fully analytical prediction (dashed lines) is clearly verified, as can be seen in the main plot. The top inset shows a collapse of both absolute values to the function  $\hbar_{\text{eff}} e^{2\lambda t}$  by calculating  $|c_{kl}^{-1} \langle k | \hat{A}(t) | l \rangle|^{2/|k-l|}$ . The bottom inset shows the deviations  $\Delta\phi_{kl} = \arg [e^{i(l-k)\phi} \langle k | \hat{A}(t) | l \rangle]$  between numerical and predicted phases (modulo  $\pi$ ) accumulated in the time evolution, with  $\phi$  defined in Eq. (12).

*Expectation values and OTOCs* — Although characterizing the time-evolution of the off-diagonal matrix elements in a given basis solves the time-dependent problem, they cannot be observed directly. Nevertheless, a direct consequence of the universal form in Eq. (1) is that expectation values are given as power series in the parameters  $\hbar_{\text{eff}} e^{2\lambda t}$ . If the system is in thermal equilibrium before the quench, this can be even refined using Wick's theorem in Eq. (15), yielding

$$\langle \hat{A}(t) \rangle = \sum_m (2m-1)! C_{2m} (\hbar_{\text{eff}} e^{2\lambda t} \langle \hat{b}_+^2 \rangle)^m, \quad (17)$$

with the temperature  $k_B T = \beta^{-1}$  entering only via

$$\langle \hat{b}_+^2 \rangle = \frac{\coth(\beta\Delta/2)}{2 \sin 2\phi}, \quad (18)$$

for  $\beta\Delta = \mathcal{O}(\hbar_{\text{eff}}^0)$ . Here,  $\Delta$  is the single-particle level spacing in the harmonic approximation, thus suggesting the further renormalization  $\hbar_{\text{eff}}^{(r)}(t, \beta) = \hbar_{\text{eff}} e^{2\lambda t} \coth(\beta\Delta/2)$ .

A common probe for the instability properties in quantum systems is the out-of-time ordered correlator (OTOC) [18, 40–43]. Using our approach one can straightforwardly obtain a multi-exponential form of the OTOC similar to a conjecture by Gu and Kitaev [44],

$$C(t) = -\langle [\hat{A}(t), \hat{B}(0)]^2 \rangle \sim (\hbar_{\text{eff}} e^{\lambda t})^2 \sum_m c_m (\hbar_{\text{eff}} e^{2\lambda t} \langle \hat{b}_+^2 \rangle)^m \quad (19)$$

with ‘classical’ coefficients  $c_m$  that are determined by the constants  $C_k$  in Eq. (15) and the linear expansion of  $\hat{B}$  in  $\hat{b}_-$ , leading to the additional factor  $\hbar_{\text{eff}}$  in Eq. (19). The OTOC scaling obtained from quasi-classical arguments [40],

$$C(t) \sim c_0 (\hbar_{\text{eff}} e^{\lambda t})^2, \quad (20)$$

corresponds only to the leading order term  $m = 0$ . One may now be tempted to use a finite number of terms in Eq. (19) to obtain a better approximation at intermediate times. However, we report here the negative result that – at least for the integrable two-site Bose-Hubbard model – the corrections are very small within the region of convergence of the series, as can be seen in the left part of Fig. 2. There, the predicted series expansion in Eq. (19) is plotted for a cutoff  $m \leq 25$  (where  $c_m = 0$  for even  $m$ ), showing a sharp breakdown at around  $t \approx 0.8t_E$ , where the leading order approximation (black dashed line) is still remarkably accurate. One should therefore not use higher-order exponentials for fitting data that do not show a clear exponential regime as was already noticed for the Sachdev-Ye-Kitaev model [45], a manifestation of the nonperturbative breakdown of the exponential behavior around  $t_E$ .

One may, however, improve the prediction in the short-time regime  $\lambda t \sim 1$  by using the full time-dependence of the leading order in  $\hbar_{\text{eff}}$ , as is demonstrated by an analytic prediction [37] (dashed black line) in Fig. 2, accurate also at early times. This may allow for well-controlled fitting in many cases where  $\hbar_{\text{eff}} = N^{-1}$  cannot be chosen arbitrarily small (c.f., [18, 46–50]).

The higher orders are, however, essential when it comes to cumulants of operators, as the  $n$ -th cumulant of an operator of the form (15) dominantly scales as [37]

$$\kappa_n(t) \sim d_n (\hbar_{\text{eff}} e^{2\lambda t} \langle \hat{b}_+^2 \rangle)^{n-1} \quad (21)$$

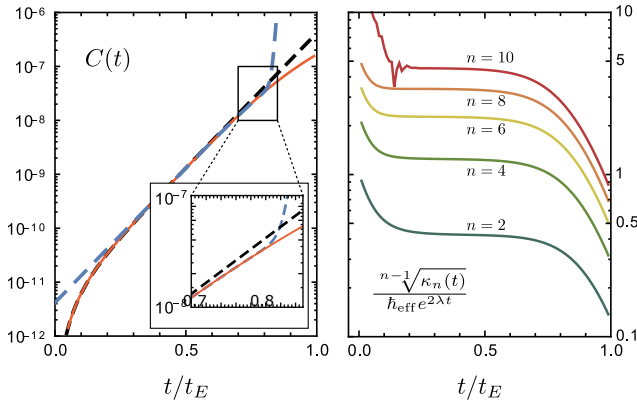


FIG. 2. Left: OTOC  $C(t) = -\langle[\hat{A}(t), \hat{B}]^2\rangle$  (solid red) for  $\hat{A} = \hat{B} = \hat{z}$  and the analytical prediction using the series expansion in the renormalized effective Planck constant (dashed blue). Dashed black line shows the analytic prediction for the leading orders including short-time corrections. Right: Numerical check of the predicted behavior of the cumulants  $\kappa_n(t)$ , Eq. (21), for  $n = 2, 4, 6, 8, 10$  using roots. The oscillations for  $n = 10$  at short times are an artifact of the finite numerical precision. All data is for  $N = 10^5$  and  $\alpha = 2.5$  with a pre-quench ( $\alpha = 0$ ) temperature  $k_B T = 2\Delta$ .

with a constant  $d_n$ . Note that the  $n$ -th moments are expected to grow only as  $(\hbar_{\text{eff}} e^{2\lambda t})^m$  with  $m = n/2$  or  $m = (n+1)/2$  for even/odd  $n$ , such that various leading order terms have to cancel in the cumulants for  $n \geq 4$ . Equation (21) is verified in the right part of Fig. 2, where numerical results for the first five non-vanishing cumulants of  $\hat{z}(t)$  are shown to follow such scaling while verifying  $\hbar e^{2\lambda t}$  as the single relevant expansion parameter for this system.

*Generalization to more degrees of freedom* — Our analysis of the two-site model can be directly generalized to systems with more degrees of freedom that have a (symmetry protected) fixed point that undergoes a bifurcation at some critical coupling, yielding

$$\hat{A}(t) \sim \sum_{\vec{k}} C_{\vec{k}} \prod_i \left( \sqrt{\hbar_{\text{eff}}} e^{\lambda_i t} \hat{b}_{\pm}^{(i)} \right)^{k_i}, \quad (22)$$

with index  $i$  running through all the unstable directions characterized through  $\hat{b}_{\pm}^{(i)}$  and the  $\lambda_i$  are the respective MF divergence rates. The connection to the matrix elements is not as straightforward in general, as the relation between the operators  $\hat{b}_{\pm}^{(i)}$  and the bosonic operators characterizing the pre-quench stable dynamics can be any linear transformation, but the largest divergence rate will generically dominate the cumulants and expectation values. The Bose-Hubbard model with  $L$  sites is special in this respect, as the interaction only enters as a quadratic term in the MF Hamiltonian, enabling a complete separation of the linearized dynamics that does not depend

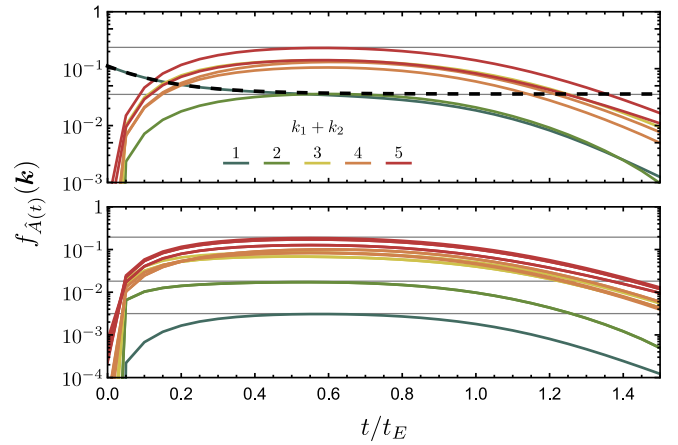


FIG. 3. Collapse of the absolute values of the non-vanishing matrix elements  $\langle k_1 k_2 | \hat{A}(t) | 0 \rangle$  for  $\hat{A}(t) = \hat{n}_1(t)/N$  (top) and  $\hat{A}(t) = [\hat{n}_1(t), \hat{n}_2(0)]/N^{3/2}$  (bottom). Each color represents a value of the sum  $k_1 + k_2$  of the quantum numbers. Thin gray horizontal lines representing the exponential predictions have been added to guide the eye. The dashed black line is the fully analytical prediction for  $(k_1, k_2) = (1, 0)$ , showing that the short-time corrections to the asymptotic exponential form are still important for  $N = 300$  particles, but the tendency towards the predicted multi-exponential behavior is clear, and gets even more evident for the commutator (bottom).

on the interaction [37], allowing also to write

$$\langle \mathbf{k} | \hat{A}(t) | \mathbf{l} \rangle \sim c_{\mathbf{k}\mathbf{l}} \prod_i \left( \sqrt{\hbar_{\text{eff}}} e^{\lambda_i t} \right)^{|k_i - l_i|} \quad (23)$$

in the basis of the pre-quench eigenstates that is selected through an infinitesimal interaction.

To show that the approach remains equally valid in systems without an integrable MF limit, a numerical simulation of the 3-site Bose-Hubbard model

$$\hat{\mathcal{H}} = -J \sum_{j=1}^3 (\hat{a}_j^\dagger \hat{a}_{j+1} + \hat{a}_{j+1}^\dagger \hat{a}_j) + \frac{U}{2} \sum_{j=1}^3 (\hat{a}_j^\dagger)^2 (\hat{a}_j)^2 \quad (24)$$

with periodic boundary conditions has been performed for  $N = 300$  particles and for an interaction quench from  $U = 0$  to  $U = -20J/N$ . The MF analysis shows a bifurcation of the global energy minimum at  $U = -9J/2N$  with two unstable directions having the same divergence rate  $\lambda$  [37].

To verify the scaling of the matrix elements, Fig. 3 shows a collapse of the (non-vanishing) matrix elements to horizontal lines using the ansatz

$$f_{\hat{A}(t)}(\mathbf{k}) = \frac{|\langle k_1 k_2 | \hat{A}(t) | 0 \rangle|_{k_1+k_2}}{\hbar_{\text{eff}} e^{2\lambda t}} \sim \text{const} \quad (25)$$

for operators satisfying the scaling (23). The upper panel uses  $\hat{A}(t) = \hat{z}_1(t)$ , where  $\hat{z}_i = \hat{n}_i/N$  is the (scaled) number operator on site  $i$ . The analytic prediction for

$k_1 + k_2 = 1$  that includes short-time corrections [37] is shown as a dashed black line and demonstrates that the deviations from exponential growth can be well explained by the fact that the requirement  $t_E = \log N/2\lambda \gg \lambda^{-1}$  is not satisfied for  $N = 300$ . The lower panel demonstrates that also the commutator of the number operators at different sites and different times has a scaling similar to Eq. (23). For this, the ansatz (25) with  $\hat{A}(t) = [\hat{z}_1(t), \hat{z}_2(0)]/\sqrt{\hbar_{\text{eff}}}$  is plotted for all excitations with  $k_1 + k_2 \leq 5$ . The factor  $\hbar_{\text{eff}}^{-1/2}$  has been introduced to correct for  $[\hat{b}_+^{(i)}, \hat{z}_i] \propto \hbar_{\text{eff}}^{1/2}$ . As can be seen in Fig. 3, the individual curves clearly approach horizontal lines in a regime between  $\lambda^{-1} \approx 0.35t_E$  and  $t_E$ .

*Conclusions* — We have developed a general framework that shows how the relevant parameter for the dynamics after a quench across a critical point is given by a renormalized effective Planck constant  $e^{2\lambda t}/N$  in the quasiclassical regime  $N \gg 1$  and for  $\lambda t \gg 1$ . We support our analytical results by extensive numerical simulations for two exemplary critical scenarios: the self-trapping transition characteristic of integrable Josephson-like Hamiltonians, and the nonintegrable three-site Bose-Hubbard model. While our approach is applicable to any system with bosonic order parameter in a well defined mean-field limit, for these specific examples we uncover the predicted scaling in the matrix elements of generic operators. Although most observables are dominated by the first-order quasi-classical result, higher-order terms in the renormalized parameter are crucial when considering cumulants of simple operators, demonstrating the quantum nature of the results.

Although some results of this letter on observables may also be obtained using other non-equilibrium methods (e.g., Keldysh field theory), the method used here directly addresses the short-time transient regime after a quench and is generally valid in any situation where a quantum-classical correspondence can be constructed. This may path the way to generalize our results to prototype examples of chaotic or mixed (many-body) systems by restricting the dynamics to the vicinity of dominant classical periodic orbits [43, 51], hence replacing unstable fixed points by (short) unstable periodic orbits with dominant short-time divergence rates.

We acknowledge funding through the Studienstiftung des Deutschen Volkes (BG) and the Deutsche Forschungsgemeinschaft through project Ri681/14-1. We thank Q. Hummel for useful conversations.

---

[1] E. Wigner, *Phys. Rev.* **40**, 749 (1932).  
 [2] R. J. Glauber, *Quantum Theory of Optical Coherence* (Viley-VCH Verlag, 2007).  
 [3] W. H. Zurek, *Rev. Mod. Phys.* **75**, 715 (2003).  
 [4] K. Richter, *Semiclassical Theory of Mesoscopic Quantum*

*Systems*, Springer Tracts in Modern Physics, Vol. 161 (Springer-Verlag Berlin Heidelberg, 2000).  
 [5] M. Brack and R. K. Bhaduri, *Semiclassical Physics*, Frontiers in Physics (Westview Press, Boulder, 2003).  
 [6] K. Hornberger, S. Gerlich, P. Haslinger, S. Nimmrichter, and M. Arndt, *Rev. Mod. Phys.* **84**, 157 (2012).  
 [7] A. Polkovnikov, *Ann. Phys.* **325**, 1790 (2010).  
 [8] R. P. Rundle, T. Tilma, J. H. Samson, V. M. Dwyer, R. F. Bishop, and M. J. Everitt, *Phys. Rev. A* **99**, 012115 (2019).  
 [9] A. Sinatra, C. Lobo, and Y. Castin, *J. Phys. B: At. Mol. Opt. Phys.* **35**, 3599 (2002).  
 [10] A. A. Norrie, R. J. Ballagh, and C. W. Gardiner, *Phys. Rev. A* **73**, 043617 (2006).  
 [11] P. Deuar and P. D. Drummond, *Phys. Rev. Lett.* **98**, 120402 (2007).  
 [12] P. Blakie, A. Bradley, M. Davis, R. Ballagh, and C. Gardiner, *Adv. Phys.* **57**, 363 (2008).  
 [13] Y. Fujiwara, T. A. Osborn, and S. F. J. Wilk, *Phys. Rev. A* **25**, 14 (1982).  
 [14] Quasiclassical refers to neglecting interfering classical solutions.  
 [15] A. Chatterjee, *Phys. Rep.* **186**, 249 (1990).  
 [16] T. Zibold, E. Nicklas, C. Gross, and M. K. Oberthaler, *Phys. Rev. Lett.* **105**, 204101 (2010).  
 [17] A. Polkovnikov, K. Sengupta, A. Silva, and M. Vengalattore, *Rev. Mod. Phys.* **83**, 863 (2011).  
 [18] S. Pappalardi, A. Russomanno, B. Žunković, F. Iemini, A. Silva, and R. Fazio, *Phys. Rev. B* **98**, 134303 (2018).  
 [19] A. Mitra, *Annu. Rev. Condens. Matter Phys.* **9**, 245 (2018).  
 [20] C. Emary and T. Brandes, *Phys. Rev. E* **67**, 066203 (2003).  
 [21] M. A. Caprio, P. Cejnar, and F. Iachello, *Ann. Phys.* **323**, 1106 (2008).  
 [22] V. M. Bastidas, P. Pérez-Fernández, M. Vogl, and T. Brandes, *Phys. Rev. Lett.* **112**, 140408 (2014).  
 [23] P. Stránský, M. Macek, and P. Cejnar, *Ann. Phys.* **345**, 73 (2014).  
 [24] M. A. Bastarrachea-Magnani, S. Lerma-Hernández, and J. G. Hirsch, *J. Stat. Mech. Theory Exp.* **2016**, 093105 (2016).  
 [25] D. Rubeni, J. Links, P. S. Isaac, and A. Foerster, *Phys. Rev. A* **95**, 043607 (2017).  
 [26] Q. Hummel, B. Geiger, J. D. Urbina, and K. Richter, *Phys. Rev. Lett.* **123**, 160401 (2019).  
 [27] M. C. Gutzwiller, *Chaos in Classical and Quantum Mechanics*, Interdisciplinary Applied Mathematics (Springer, New York, 1990).  
 [28] B. V. Chirikov, F. Izrailev, and D. Shepelyansky, *Sov. Scient. Rev. C* **2**, 209 (1981).  
 [29] J. Rammensee, J. D. Urbina, and K. Richter, *Phys. Rev. Lett.* **121**, 124101 (2018).  
 [30] B. Juliá-Díaz, D. Dagnino, M. Lewenstein, J. Martorell, and A. Polls, *Phys. Rev. A* **81**, 023615 (2010).  
 [31] P. Kunkel, M. Prüfer, S. Lannig, R. Rosa-Medina, A. Bonnin, M. Gärttner, H. Strobel, and M. K. Oberthaler, *Phys. Rev. Lett.* **123**, 063603 (2019).  
 [32] K. Nemoto, C. A. Holmes, G. J. Milburn, and W. J. Munro, *Phys. Rev. A* **63**, 013604 (2000).  
 [33] R. Franzosi and V. Penna, *Phys. Rev. E* **67**, 046227 (2003).  
 [34] N. Oelkers and J. Links, *Phys. Rev. B* **75**, 115119 (2007).  
 [35] R. Kanamoto, H. Saito, and M. Ueda, *Phys. Rev. Lett.*

- [94](#), 090404 (2005).
- [36] L. Khaykovich, F. Schreck, G. Ferrari, T. Bourdel, J. Cubizolles, L. D. Carr, Y. Castin, and C. Salomon, *Science* **296**, 1290 (2002).
- [37] B. Geiger, See Supplemental Material at [URL](#) for the mean-field analysis of the BH dimer and the BH model with  $L$  sites, for the proof of Eq. (4) and the calculation of the coefficients  $c_{kl}$  for harmonic oscillator states and the generalization to general eigenstates, including explicit short-time first-order results used in Figs. 2 and 3.
- [38] J. D. Franson and M. M. Donegan, *Phys. Rev. A* **65**, 052107 (2002).
- [39] If  $\hat{A}$  is a power series in  $\hbar_{\text{eff}}$  the result applies to the  $\hbar_{\text{eff}}$ -independent coefficients individually.
- [40] A. I. Larkin and Y. N. Ovchinnikov, *J. Exp. Theor. Phys.* **28**, 1200 (1969).
- [41] E. B. Rozenbaum, S. Ganeshan, and V. Galitski, *Phys. Rev. Lett.* **118**, 086801 (2017).
- [42] J. S. Cotler, D. Ding, and G. R. Penington, *Ann. Phys.* **396**, 318 (2018), [arXiv:1704.02979](#).
- [43] A. Lerose and S. Pappalardi, *Phys. Rev. A* **102**, 032404 (2020).
- [44] Y. Gu and A. Kitaev, *J. High Energy Phys.* **2019**, 75 (2019).
- [45] B. Kobrin, Z. Yang, G. D. Kahanamoku-Meyer, C. T. Olund, J. E. Moore, D. Stanford, and N. Y. Yao, “Many-Body Chaos in the Sachdev-Ye-Kitaev Model,” (2020), [arXiv:2002.05725](#).
- [46] N. Y. Yao, F. Grusdt, B. Swingle, M. D. Lukin, D. M. Stamper-Kurn, J. E. Moore, and E. A. Demler, “Interferometric Approach to Probing Fast Scrambling,” (2016), [arXiv:1607.01801](#).
- [47] A. Bohrdt, C. B. Mendl, M. Endres, and M. Knap, *New J. Phys.* **19**, 063001 (2017).
- [48] H. Shen, P. Zhang, R. Fan, and H. Zhai, *Phys. Rev. B* **96**, 054503 (2017).
- [49] A. Keleş, E. Zhao, and W. V. Liu, *Phys. Rev. A* **99**, 053620 (2019).
- [50] É. Lantagne-Hurtubise, S. Plugge, O. Can, and M. Franz, *Phys. Rev. Res.* **2**, 013254 (2020).
- [51] E. J. Heller, *Phys. Rev. Lett.* **53**, 1515 (1984).